Influence of Loading History on the Drift Capacity of Limited Ductile Reinforced Concrete Columns

Saim Raza[1], Scott J. Menegon[2], Hing-Ho Tsang[3] and John L. Wilson[4]

1. PhD Student, Department of Civil and Construction Engineering, Swinburne University of Technology, VIC, Australia.
   Email: sraza@swin.edu.au (Corresponding Author)

2. Research Fellow, Department of Civil and Construction Engineering, Swinburne University of Technology, VIC, Australia; and
   Senior Structural Engineer, Wallbridge Gilbert Aztec, Melbourne, VIC, Australia.
   Email: smenegon@swin.edu.au

3. Senior Lecturer, Department of Civil and Construction Engineering, Swinburne University of Technology, VIC, Australia.
   Email: htsang@swin.edu.au

4. Professor, Deputy Vice-Chancellor and Chief Executive Officer Swinburne Sarawak, Swinburne University of Technology, VIC, Australia.
   Email: jwilson@swin.edu.au

Abstract

A building column experiences complex multi-directional loading during an earthquake. The loading comprises of lateral forces in the two orthogonal horizontal axes, resulting in bidirectional bending, and variable axial loading along the vertical axis of the column. However, due to the limitation of the testing facilities, most of the experimental studies have focussed on the unidirectional behaviour of the RC column only. The aim of this paper is to evaluate the influence of the loading history on the drift capacity of reinforced concrete (RC) columns. The loading histories considered include unidirectional cyclic loading with constant axial load, bidirectional cyclic loading with constant axial load and bidirectional cyclic loading with variable axial load. To this end, the results of an experimental testing program comprising of 14 high-strength RC columns, representative of Australian construction practice and tested under different loading histories are discussed.

Keywords: Loading history, drift capacity, RC columns, limited ductility

1 Introduction

The three concurrent components of the ground motions result in varying triaxial forces on the structural elements, such as columns, during earthquakes. The triaxial forces imposed during earthquakes comprise of biaxial bending along the two horizontal axes and variable axial load along the vertical axis of the column. The simulation of these varying triaxial forces under laboratory conditions is a complex task, and therefore most of the experimental testing in the literature has approximated the response of the column under unidirectional lateral loading with constant axial load (CAL) only. Few studies (Rodrigues et al. 2013a, Ludovico et al. 2013, Chang et al. 2010) have also evaluated the response under bidirectional lateral loading with constant axial load. However, the behaviour under varying triaxial forces i.e. bidirectional lateral loading with variable axial load (VAL) has rarely been investigated (Rodrigues et al. 2013b).

Previous studies have shown that the behaviour of RC column is highly dependent on the type of loading path (Pham and Li 2013). Considering this, it is very pertinent to understand the differences in the force-displacement behaviour of the column under different earthquake loading histories. Furthermore, most of the existing studies were conducted on RC columns with detailing representative of high seismic regions. On the other hand, due to perceived lower seismic risk, limited ductile detailing with widely spaced transverse reinforcement is adopted in regions of low to moderate seismicity, which results in lower drift capacity of such columns compared to the columns with ductile detailing in regions of higher seismicity (Raza et al. 2018), thereby increasing the vulnerability of collapse of such columns in a rare or very earthquake event.

The aim of this study is to evaluate the impact of loading history on the drift behaviour of limited ductile RC columns prevalent in regions of low to moderate seismicity. To this end, a comprehensive experimental testing program was conducted in the smart structures laboratory of Swinburne University of Technology, Australia, in which limited ductile high-strength RC (HSRC) columns were tested under three different loading scenarios i.e. unidirectional lateral loading with constant axial load, bidirectional lateral loading with constant axial load and bidirectional lateral loading with variable axial load. The results in terms of the drift capacity of the specimens are presented herein.

2 Experimental Program

A total of 14 limited ductile HSRC columns were experimentally tested. The variable parameters of the study were axial load ratio, transverse reinforcement ratio, concrete compressive strength and the type of loading path. Table 1 provides brief details about the testing program. The specimens were provided with a minimum effective confining pressure of $0.01f_c'$ in accordance with deem to comply requirements of AS 3600-2018. These requirements result in limited ductile HSRC columns, and as such the scope of this study is confined to limited ductile HSRC columns. More details regarding specimen design, instrumentation and test set up can be found in Raza et al. (2019a), Raza et al. (2019b) and Raza et al. (2019c). The testing was conducted under Multi-Axial Substructure Testing (MAST) system. Figure 1 presents the design details and orientation of the specimen under the MAST system.

3 Loading Protocols

This section provides details of the loading protocols, namely unidirectional lateral loading with constant axial load, bidirectional lateral loading with constant axial load

Table 1: Details of the Experimental Program

No.	Width × Depth × Height (mm)	Concrete Mean Strength f_{cm} (MPa)	Longitudinal Reinforcement ρ_v (%)	Stirrups (mm) ρ_{hy} (%)	Axial Load Ratio n	Type of Loading Path
S1	250×300×2550	75.0	6N16(1.6%)	N10@150 (0.35%)	0.15	Uni-Directional +CAL
S2	250×300×2550	66.0	6N16(1.6%)	N10@150 (0.35%)	0.30	Uni-Directional +CAL
S3	250×300×2550	87.0	6N16(1.6%)	N10@150 (0.35%)	0.45	Uni-Directional + CAL
S4	250×300×2550	90.0	6N16(1.6%)	N10@100 (0.52%)	0.45	Uni-Directional +CAL
S5	250×300×2550	62.0	6N16(1.6%)	N10@300 (0.18%)	0.30	Uni-Directional +CAL
S6	250×300×2450	90.0	6N16(1.6%)	N10@150 (0.35%)	0.25	Uni-Directional + CAL
S7	250×300×2550	86.0	6N16(1.6%)	N10@150 (0.35%)	0.15	Bi-Directional (Linearised Circular 1:1) + CAL
S8	250×300×2550	63.0	6N16(1.6%)	N10@150 (0.35%)	0.30	Bi-Directional (Linearised Circular 1:1) + CAL
S9	250×300×2550	90.0	6N16(1.6%)	N10@150 (0.35%)	0.15	Bi-Directional (Octo-Elliptical 1:1) + CAL
S10	250×300×2550	83.0	6N16(1.6%)	N10@150 (0.35%)	0.30	Bi-Directional (Octo-Elliptical 1:1) + CAL
S11	250×300×2550	105.0	6N16(1.6%)	N10@150 (0.35%)	0.15	Bi-Directional (Octo-Elliptical 1:0.6) + CAL
S12	250×300×2550	74.0	6N16(1.6%)	N10@150 (0.35%)	0.30	Bi-Directional (Octo-Elliptical 1:0.6) + CAL
S13	250×300×2550	87.0	6N16(1.6%)	N10@150 (0.35%)	0.15±0.045	Bi-Directional (Octo-Elliptical 1:0.6) + SS-VAL
S14	250×300×2550	85.0	6N16(1.6%)	N10@150 (0.35%)	0.15±0.045	Bi-Directional (Octo-Elliptical 1:0.6) + NS-VAL

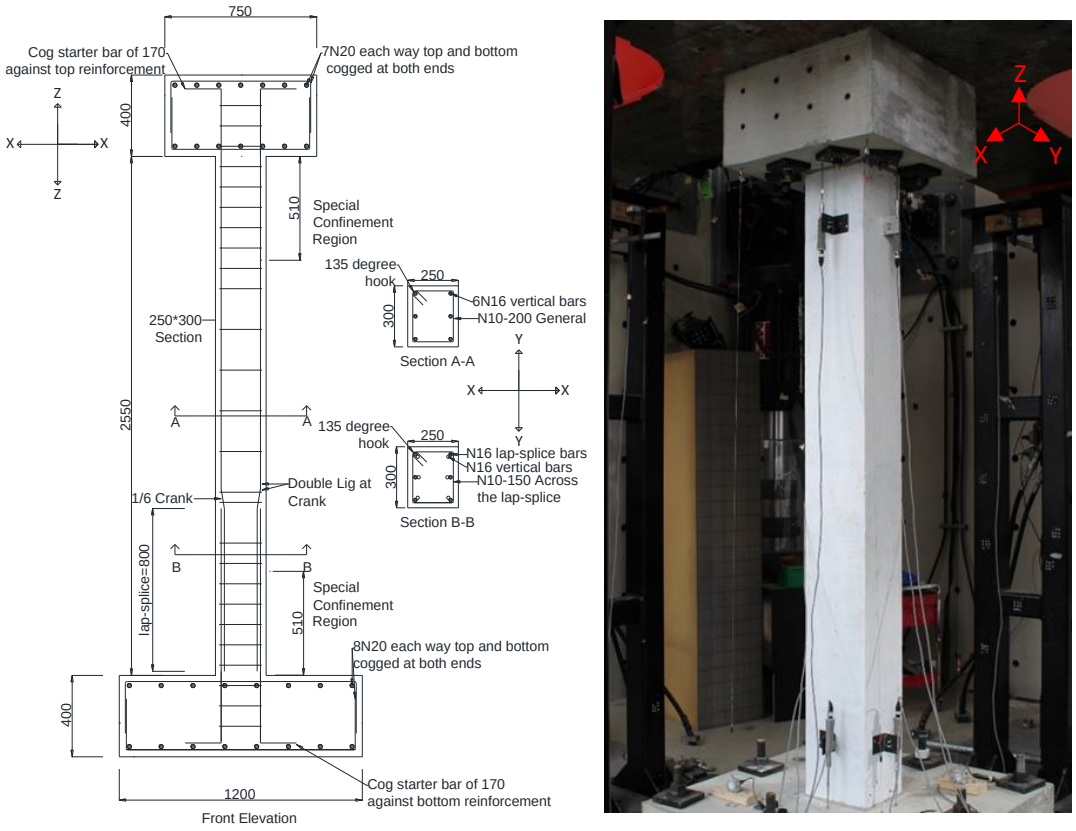

(a) (b)

Figure 1 (a) Details of RC column (mm) (b) Specimen under multi-axial substructure testing (MAST) facility

and bidirectional lateral loading with variable axial load used in the testing program.

3.1 Unidirectional Lateral Loading with Constant Axial Load

In this loading protocol, an axial load was first applied at the top pedestal via cross-head of the Multi-Axial Substructure Testing (MAST) system and was maintained constant throughout the duration of the test. The specimens were then subjected to quasi-static incrementally increasing displacements in the stronger (Y-axis) direction as summarized in Figure 2. Each displacement excursion was repeated twice to capture the strength degradation behaviour of the column. The displacement of the first and second loading cycles was equal to approximately 0.5 and 1.0 times the theoretical yield drift, respectively. All the subsequent cycles had a displacement increment between 5/4 and 3/2 times of the displacement excursion of the preceding cycle, in accordance with the recommendations of ACI ITG-5.1-07 (ACI ITG 2008).

Six specimens were tested under this loading protocol. The testing was stopped when the axial load failure of the column occurred (i.e. the column could no longer support the initially applied axial load).

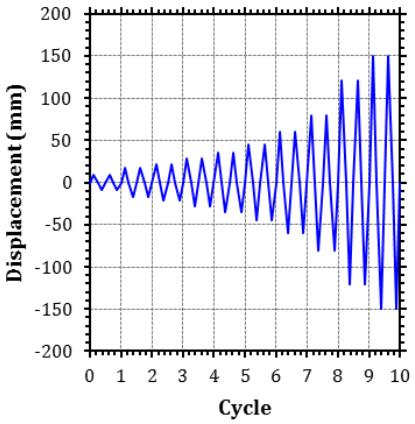

Figure 2. Displacement controlled unidirectional cyclic lateral load history

3.2 Bidirectional Lateral Loading with Constant Axial Load (CAL)

The specimens were tested under constant axial load and bidirectional lateral actions in this protocol. Three different bidirectional loading protocols, namely the linearised circular path (1:1), octo-elliptical path (1:1) and octo-elliptical path (1:0.6) were adopted for this study.

The linearised circular path shown in Figure 3 (a) consists of a quarter of a circle in each quadrant. Each quarter-circle starts and finishes at the origin. The column is first displaced in the first quadrant, followed by displacement in the third, second and fourth quadrants, respectively, before finishing back at the origin. After completion of one cycle of quarter circles, the specimen is subjected to the second cycle of quarter circles in all quadrants for capturing the strength and stiffness degradation under repeated displacement excursions, thereby resulting in a total of 8 quarter circles of loading per displacement increment.

The octo-elliptical (1:1) loading path, shown in Figure 3 (b), is a more sophisticated bidirectional loading protocol, which attempts to generalize the actual displacement path of the column during an earthquake ground motion using elliptical loops of different orientations. The octo-elliptical path is comprised of four elliptical loops, which are each repeated twice, resulting in eight loading loops per displacement increment. The first four loops displace the column in the counter-clockwise direction and the last four displace it in the clockwise direction. The aspect ratio (a/b) of the individual ellipses (i.e. loops) is 1:0.3 and the ratio of the overall enveloped strong to weak axis (y/x) displacement is 1:1, which means the column is subjected to equal displacement in the strong and weak directions. As such, all the individual ellipses are circumscribed within a circular path. The octo-elliptical path (1:1) begins with a vertical ellipse that displaces the column in the Y-direction (strong-axis) from the origin. This is followed by diagonal displacement via diagonal ellipse, and then horizontal displacement in the X-direction (weak-axis) through a horizontal ellipse. Finally, the fourth and the last ellipse of the counter-clockwise cycle displaces the column diagonally again before bringing it back to the origin. After finishing one complete cycle of displacements in the counter-clockwise direction, the four ellipses are repeated again but this time in the clockwise direction. In this loading protocol, a smooth transition is provided from one ellipse to another using arcs. The two small semi-circles visible around the origin are due to these arcs. The upper semicircle is formed when the ellipses are moving in the counter-clockwise direction, whereas lower semicircle is formed during the displacement in the clockwise direction.

The octo-elliptical (1:0.6) loading path shown in Figure 3 (c), on the other hand, is the same as the octo-elliptical (1:1) path except that the ratio of the overall enveloped strong to weak axis displacement of the column is 1:0.6, thereby circumscribing (enveloping) the individual ellipses within an elliptical path instead of a circular one.

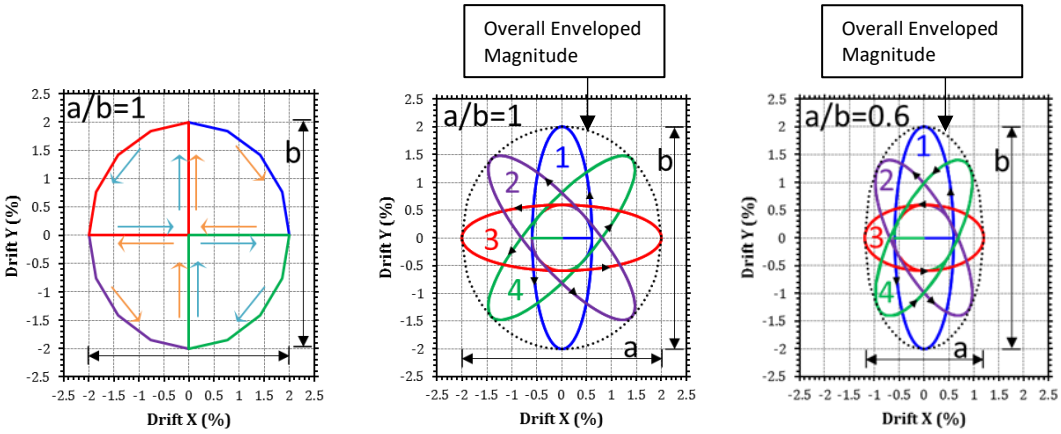

Figure 3. Displacement controlled bidirectional lateral loading protocols a) linearised circular (1:1) path b) octo-elliptical (1:1) path c) octo-elliptical (1:0.6) path

A total of 6 specimens, two under each of the three presented bidirectional protocols, were tested till the axial load failure of the column (i.e. the point when column could no longer support the initially applied axial load).

3.3 Bidirectional Lateral Loading with Variable Axial Load (VAL)

Two specimens were tested under bidirectional lateral loading with variable axial load. The bidirectional loading protocol used was octo-elliptical (1:0.6) path for both the specimens. The specimens were tested with a 'baseline' axial load of n=0.15 with a variation of ±30% during the testing, which resulted in an axial load ratio of 0.15 ± 0.045 across the duration of the testing. Two different axial load variation protocols were employed in this study. The first protocol is referred to as *synchronous axial load variation* protocol as it was synchronous with the lateral displacement in the strong direction (Y-axis) of the column as shown in Figure 4. It can be observed in Figure 4 (a) that axial load is maximum when the lateral displacement is maximum in the positive direction and minimum when the lateral displacement is maximum in the negative direction. On the other hand, due to the phase shift in the displacements of X and Y directions, Figure 4 (b) indicates that axial load variation is slightly nonsynchronous with the displacements in the X-direction. This is because axial load variation is primarily a function of displacements in the strong direction (Y-axis) of the column, which are greater than the displacements in the weak direction (X-axis).

The second protocol is referred to as *nonsynchronous axial load variation* protocol in which there were two cycles of axial load variation per one cycle of lateral displacement as shown in Figure 5. Under nonsynchronous loading protocol, in the strong direction of the column, axial load reached its maximum value whenever the column was pushed to its maximum amplitude of displacement either in the positive or negative direction and minimum value when the column was at the origin (i.e. stationary). This is in contrast with the synchronous loading protocol in which the column was subjected to maximum axial load when maximum amplitude of displacement was attained in the positive (strong) direction and minimum axial load when amplitude of displacement was maximum in the negative (strong) direction. On the other hand, in the weak direction of the column, under nonsynchronous loading protocol, the axial load ratio

was mostly at its minimum value when the displacement was maximum in either direction and was mostly maximum when the column was at the origin.

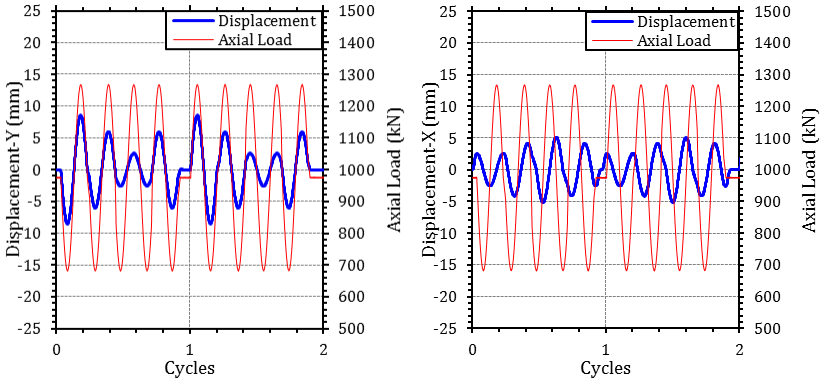

(a) (b)

Figure 4. Synchronous axial load variation protocol a) Y-axis b) X-axis

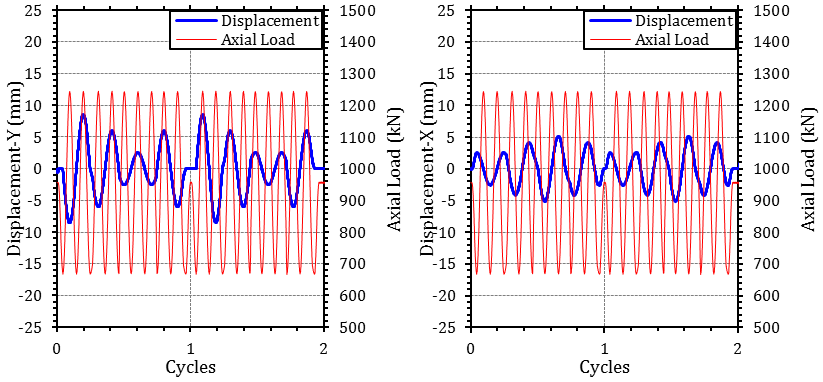

(a) (b)

Figure 5. Nonsynchronous axial load variation protocol a) Y-axis b) X-axis

4 Drift Capacity

Strong Axis

The comparison of drift capacity in the Y-direction (Strong Axis) of the specimens under different loading histories is presented in Figure 6. It is noted that lateral load failure drift here refers to the drift capacity corresponding to 20% degradation in the lateral strength and axial load failure drift refers to the drift capacity corresponding to the loss of axial load carrying capacity of the column (i.e. when column fails to support the initially applied axial load). The comparison of drift behaviour of unidirectional and bidirectional loading paths with constant axial load is presented here first.

It can be observed in Figure 6 that there is a significant reduction in the lateral and axial load failure drift capacity of the column under bidirectional loading paths with constant axial load i.e. Octo-Elliptical (1:0.6) + CAL and Octo-Elliptical (1:1) + CAL loading paths, in contrast with the unidirectional loading path with CAL. The uniaxial lateral load failure drift of the column reduced by 25% and 40% under octo-elliptical (1:0.6) + CAL and octo-elliptical (1:1) + CAL loading histories, respectively, at n=0.15 and reduced by 35% and 50%, respectively, at n=0.3. Similarly, the uniaxial axial load failure drift capacity of the column reduced by 36% and 50% under octo-elliptical (1:0.6) and octo-elliptical (1:1) loading paths, respectively, at n=0.15, and reduced by 40% and 56%, respectively, at n=0.3 for the same loading histories.

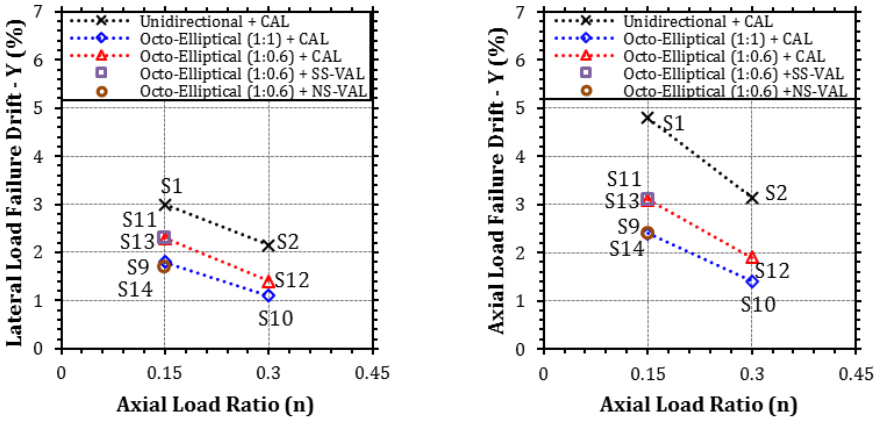

(a) (b)

Figure 6. Effect of loading path on the drift capacity (strong axis loading) of the column a) lateral load failure drift b) axial load failure drift

A comparison of the drift behaviour of the specimens under bidirectional loading with constant axial load and bidirectional loading with variable axial load in Figure 6 indicates that drift capacity of the specimen is similar for octo-elliptical (1:0.6) path with constant axial load and octo-elliptical (1:0.6) path with synchronous variable axial load. However, the lateral load failure and axial load failure drifts of the specimen tested under octo-elliptical (1:0.6) path with nonsynchronous variable axial load are about 25% lower than the corresponding specimen tested under octo-elliptical (1:0.6) path with constant axial load. It is also noteworthy that lateral load failure and axial load failure drifts of the specimen tested under octo-elliptical (1:0.6) path with nonsynchronous variable axial load were similar to the drift capacity exhibited by specimen tested under octo-elliptical (1:1) with constant axial load. This implies that nonsynchronous axial load variation with smaller enveloped bidirectional lateral loading i.e. 1:0.6 along the two axes of the specimen has the same impact on the drift capacity of the column in the strong axis as bidirectional lateral loading (under constant axial load) with larger enveloped displacements i.e. 1:1 along the two-axis.

It is noted that the drift results of the specimen tested under linearised circular path (1:1) with constant axial load were identical to the specimen tested under octo-elliptical (1:1) path with constant axial load, and are thus not discussed herein. However, this implies that the drift capacity of the column is not overly dependent on the path of displacement in a loading protocol but is more dependent on the overall enveloped magnitude of displacements in the strong and weak axis of the column.

Weak Axis

The effect of different loading paths on the lateral load failure and axial load failure drift capacity in the weak axis of the specimens is shown in Figure 7. As it would be expected, the drift capacity of the specimens tested under protocol with larger enveloped displacements i.e. octo-elliptical (1:1) path and CAL, was about 20-25% more in the weak axis compared to the specimens tested under protocol with smaller enveloped displacement i.e. octo-elliptical (1:0.6) path and CAL. This is because under octo-elliptical (1:0.6) loading history, failure is controlled by the drift in the strong axis of the column, which is greater than the other axis, whereas under octo-elliptical (1:1) loading path failure is controlled by drift in both the major and minor axis of the specimen (because they are equal in the loading protocol).

The lateral load failure drift of the specimens tested under octo-elliptical (1:0.6) loading path with constant and variable (both synchronous and nonsynchronous) axial load was found to be same in the weak axis, whereas axial load failure drift under nonsynchronous variable axial loading history was about 20% less than synchronous variable and constant axial loading histories. This means that nonsynchronous axial load variation loading protocol results in the most reduction of the drift capacity.

A comparison could not be made between the unidirectional and bidirectional drift capacity of the column in the weak axis as tests were not conducted to evaluate the uniaxial drift capacity of the specimen along the weak axis.

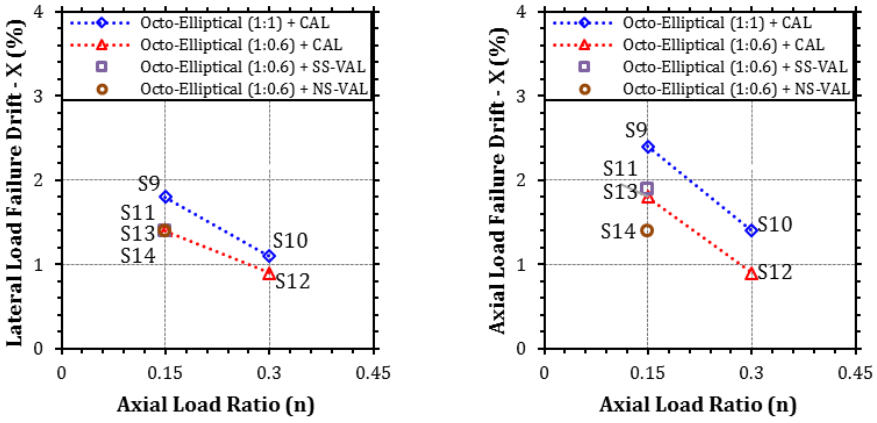

(a) (b)

Figure 7. Effect of loading path on the drift capacity (minor axis loading) of the column a) lateral load failure drift b) axial load failure drift

5 Conclusion

This paper presented a comparative assessment of the drift capacity of limited-ductile RC columns under different axial and lateral loading histories. The results of the experiments demonstrated that drift capacity of the specimens can reduce by approximately 50% when subjected to bidirectional loading as opposed to unidirectional lateral loading. It was also found that the drift capacity of the column is dependent on the strong to weak axis displacement ratio of the column. As such, the uniaxial failure drift capacity in the strong axis of the column reduced by 50% and 36% when the ratio of displacements were 1.0 and 0.6, respectively, regardless of the type of loading path used. This means that drift capacity of the column is not overly dependent on the type of bidirectional loading path but rather more dependent on the overall enveloped magnitude of displacements in a bidirectional loading path. Hence, the drift capacity of two similar columns will be almost identical if they are tested under two different bidirectional loading paths, where the column is pushed to the same magnitude of enveloped displacements along the two axes. The experimental results also showed that bidirectional lateral loading with nonsynchronous variable axial load results in the lowest drift capacity of the RC column. On the other hand, bidirectional lateral loading with synchronous variable axial load and constant axial load result in similar drift capacity of the column.

Acknowledgement

The authors greatly acknowledge Bushfire and Natural Hazards CRC for providing financial support and Swinburne Smart Structures Lab staff for providing technical assistance to conduct this experimental testing program successfully.

References

ACI (American Concrete Institute). (2008). Acceptance criteria for special unbonded post-tensioned precast structural walls based on validation testing and commentary. ACI ITG-5.1-07, Farmington Hills, MI.

AS 3600-2009 Concrete Structures. Standards Australia.

Chang S.Y. (2010). Experimental studies of reinforced concrete bridge columns under axial load plus biaxial bending. Journal of Structural Engineering 136(1), pp. 12-25.

Ludovico M.D., Verderame G.M., Prota A., Manfredi G., Cosenza E (2013). Experimental behavior of nonconforming RC columns with plain bars under constant axial load and biaxial bending. Journal of Structural Engineering. 139(6), pp. 897-914.

Pham, T. P., Li, B. (2013). Seismic behaviour of reinforced concrete columns with light transverse reinforcement under different lateral loading directions. ACI Structural Journal, 110, pp. 833-843.

Raza, S., Tsang, H.H., Wilson, J.L., (2018), Unified models for post-peak failure drifts of normal- and high-strength RC columns, Magazine of Concrete Research, 70(21), pp. 1081-1101

Raza S., Menegon S.J., Tsang H.H., Wilson J.L (2019a). Collapse performance of limited ductile high-strength RC columns under uni-directional cyclic actions. Journal of Structural Engineering (Under Review).

Raza S., Menegon S.J., Tsang H.H., Wilson J.L (2019b). Force-displacement behaviour of limited ductile high-strength RC columns under bidirectional earthquake actions. Engineering Structures (Under Review).

Raza S., Menegon S.J., Tsang H.H., Wilson J.L (2019c). Axial load variation of limited ductile high-strength RC columns subject to bidirectional lateral loading. Journal of Earthquake Engineering (Under preparation).

Rodrigues H., Arêde A., Varum H., Costa A.G (2013a). Experimental evaluation of rectangular reinforced concrete column behavior under biaxial cyclic loading. Earthquake Engineering and Structural Dynamics, 42(2), pp. 239-259.

Rodrigues, H., Varum, H., Arêde, A., Costa, A. G. (2013b). Behaviour of reinforced concrete column under biaxial cyclic loading—State of the Art. International Journal of Advanced Structural Engineering, 5(4).